

Deterministic versus stochastic modelling of unsaturated flow in a sandy field soil based on dual tracer breakthrough data

Gunnar NÜTZMANN^{1, 2}, Stanisław MACIEJEWSKI³
and Wioletta GORCZEWSKA-LANGNER^{4, *}

¹ Leibniz-Institute of Freshwater Ecology and Inland Fisheries, Müggelseedamm 310, D-12587 Berlin, Germany

² Humboldt-University of Berlin, Germany and Geographical Department, Unter den Linden 6, D-10099 Berlin, Germany

³ Institute of Hydroengineering of Polish Academy of Sciences, Kościarska 7, 80-828 Gdańsk, Poland

⁴ Gdańsk University of Technology, Faculty of Civil and Environmental Engineering, Narutowicza 11/12, 80-233 Gdańsk, Poland; ORCID: 0000-0001-9907-552



Nützmann, G., Maciejewski S., Gorczevska-Langner, W., 2022. Deterministic versus stochastic modelling of unsaturated flow in a sandy field soil based on dual tracer breakthrough data. *Geological Quarterly*, 2022, 66: 37, doi: 10.7306/gq.1669

Associate Editor: Beata Jaworska-Szulc

The 216 km² Neuenhagen Millcreeck catchment can be characterized as a drought-sensitive landscape in NE Germany. It is therefore of fundamental human interest to understand how water that fell as precipitation moves through the unsaturated soils and recharges groundwater. Additionally, a better knowledge of nutrient transport from soil to groundwater is important, especially in landscapes with light sandy soils. For a better understanding of these processes a dual tracer field experiment with bromide (Br⁻) and deuterium (D₂O) was carried out some years ago. The aim of the present study is to use the results of this experiment to model tracer transport in the unsaturated zone via two different concepts, the classical deterministic advection-dispersion equation and a new stochastic approach. The advantage of the stochastic modelling method proposed here for field-scale tracer application is to produce reliable information about expected total solute fluxes from the unsaturated zone to groundwater and about mean transit times. Moreover, this allows one to evaluate the mass of solute in the soil profile and to determine the range of water velocity fluctuations. Field experiments should be concentrated on estimation of fluctuation of water flow velocity to make stochastic models more accurate. To summarize, this work contributes to new modelling methods for the simulation of water and solute transport in unsaturated sandy soils which are heavily affected by droughts and irregular hydrological processes in the subsurface.

Key words: unsaturated flow, tracer transport, breakthrough curve, deterministic modelling, stochastic modelling.

INTRODUCTION

Experiments concerning solute movement through the unsaturated zone show significant fluctuations of soil water velocity and provide evidence for the existence of many flow paths in the soil profile. In a large-scale field experiment, Biggar and Nielsen (1976) observed solute movement under twenty ponded plots located randomly over a 150 ha field. They found that the velocity of the solute peak was distributed lognormally with a large coefficient of variation of 194%. In other studies (Butters et al., 1989; Hammel et al., 1999; Wessolek et al., 2000; Moroni et al., 2007) similar processes have been mea-

sured and quantified. Nützmann and Maciejewski (2002) and Nützmann et al. (2002) have shown that even for a homogeneous unsaturated soil column, significant fluctuation of water velocity can occur depending on the degree of water saturation. It is recognized that solute dispersivity increases with the scale of the transport medium (Fried, 1975; Yeh, 1987). This effect of increasing dispersivity for long saturated columns was also reported by Huang et al. (1995) and Xiong et al. (2006). Pachepsky et al. (2000) described transport assuming that the random movement of solute particles belongs to the family of so-called Levy motions.

In summary, solute transport in unsaturated porous media at the field scale is very complex and several studies have shown that the advection-dispersion equation cannot correctly describe the phenomena observed. These phenomena are referred to as non-Fickian or anomalous dispersion (Berkowitz and Scher, 1995; Bromly and Hinz, 2004; Cortis and Berkowitz, 2004; Raimbault et al., 2021; Li et al., 2021).

Due to soil heterogeneity, Dagan and Bresler (1979) proposed a stochastic description of transport in soil. Since the spa-

* Corresponding author, e-mail: wiogorc@pg.edu.pl

Received: May 25, 2022; accepted: November 16, 2022; first published online: December 30, 2022

tial distribution of the various parameters (hydraulic conductivity at saturation, rate of recharge, solute initial concentration etc.) is affected by uncertainty, they proposed to regard them as random space functions (RSFs). Thus, these variables are characterized by joint probability density functions (PDFs). Consequently, the flow and transport variables of interest are also RSFs and they can be determined in terms of their statistical moments only. PDFs describing field parameters can be identified from histograms of measured values. In the approach of [Dagan and Bresler \(1979\)](#) the flow is assumed to be vertical and the soil properties are averaged over the depth, such that all properties and flow variables become RSFs of the horizontal coordinates only. The above assumption of one-dimensional flow in the vertical direction, i.e., regarding the porous medium as a collection of vertical columns, considerably simplifies the modelling of flow and transport under quite general conditions of transient boundaries and complex solute behaviour. Such models, which consider water flow in the field as a set of parallel soil columns with their local advection-dispersion parameters, are called stochastic stream tube models (STMs). STMs have been used to describe solute movement in soil for various field experiments (see e.g., [Amoozegard-Fard et al., 1982](#); [Jaynes and Bowman, 1988](#); [Tilahun et al., 2005](#); [Claes et al., 2019](#)). The theoretical background of STMs has been discussed in detail by [Toride and Leij \(1996a, b\)](#), who also developed procedures for its application to both reactive and non-reactive solutes under chemical equilibrium and non-equilibrium conditions.

To understand the mechanisms of nutrient transport in the unsaturated zone as basic principles for a diffuse input of these chemicals into surface water, experimental investigations have been carried out at the Erpe River test site ([Tischner, 2000](#)). As one result, a strong dependence of leaching from subsurface hydrological conditions, i.e. short-term changes in vertical flow velocities, was detected ([Nützmann and Tischner, 2000](#)).

The aim of the present study is to use results of a dual tracer field experiment with bromide (Br^-) and deuterium (D_2O), reported in [Berg et al. \(2001\)](#), for modelling tracer transport in the unsaturated zone with two different concepts, the classical deterministic advection-dispersion equation and a new stochastic approach. In the Materials and Methods section, the field experiment is briefly described. Based on measured hydro-climatic and hydrological quantities (precipitation, tension), and estimated soil hydraulic functions, a physically-based 1D water flow

model has been applied and verified. Results show that solute transport cannot be successfully simulated using a 1D deterministic advection-dispersion model. Next, a stochastic tracer transport model based on the concept of [Chan and Govindaraju \(2006\)](#) was developed and tested against the breakthrough data. In the final section of the paper we present results that highlight the strengths and weaknesses of these methods.

MATERIAL AND METHODS

DESCRIPTION OF THE DUAL TRACER EXPERIMENT

The Erpe catchment area consists of hydraulically conductive sandy horizons in the unsaturated zone and in the unconfined aquifer (saturated hydraulic conductivity ranges from $4.5 \cdot 10^{-5}$ to $1.25 \cdot 10^{-4} \text{ m s}^{-1}$) with a thickness of 10 to 30 m. The soil cover with a thickness of between 0.15 and 0.45 m consists of fine and medium sands with a bulk density of 1.65 to 1.73 g cm^{-3} . Based on the unsaturated hydraulic properties of the unsaturated zones, four horizons could be distinguished, where porosities are between 0.31 and 0.36 ([Nützmann and Tischner, 2000](#)). The water table at the experimental site varies between 170 and 200 cm below the soil surface.

As shown in [Figure 1](#), ceramic suction cups for soil water sampling and tensiometers were arranged along the transect at six locations (I–VI) at four different depths. Around location II and III, an additional two parallel sampling points (A and B) at depths of 30 and 60 cm were installed to obtain more spatial information about soil water fluxes and tracer transport. Owing to their construction, suction cups were held under a constant pressure of 0.4 bars, so that soil water could flow into the collectors continuously. These soil water samples were taken weekly. Measurements of the concentration of tracers in the samples allowed estimation of the flow rates of groundwater and of the parameters of hydrodynamic dispersion.

At the same depths, tensiometers were used to monitor pressure head in the unsaturated zone every 60 min.

Precipitation was recorded hourly at the test site, and from daily measured hydro-meteorological quantities, evapotranspiration was calculated using the Penman-Monteith equation ([DVWK, 1996](#)). Thus, a time series of net precipitation was de-

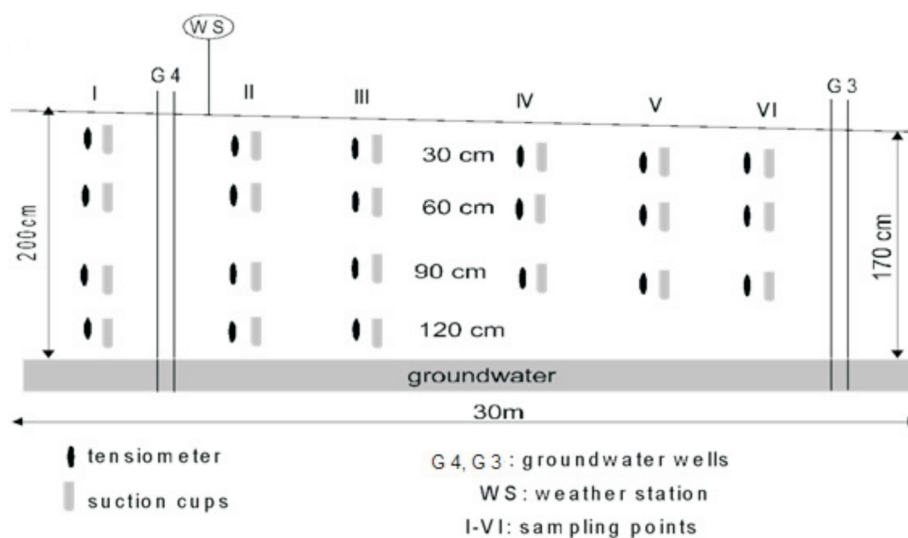


Fig. 1. Vertical cross-section of the field test site; dual tracer was applied on a 10 m^2 area around the location II

rived for the test site with a daily resolution (the cumulative net precipitation in the hydrological summer was 331, and 254 mm in the hydrological winter).

Two observation wells (G4, G3) allowed sampling of groundwater inflow and outflow of the test site, with water levels measured in one-week increments.

Tracer injection was carried out in March. The dual tracer, consisting of 60 g of sodium-bromide and 0.5 l of water containing 99.86 atom% of deuterium was dissolved in 200 l water and equally distributed over the soil surface on a 10 m² area around location II over one hour. Thus, we have initial concentrations of $c_0 = 232 \text{ mg l}^{-1}$ for bromide, and, $c_0 = 2771 \text{ mg l}^{-1}$ for water traced by deuterium.

The amount of irrigated water (20 mm) corresponds to a normal spring rainfall event. Because of the climatic conditions in March, it can be assumed that evaporation did not occur during the tracer application. During the very dry summer months there is a long stagnant period without detectable water movement in the unsaturated zone, thus soil water samples were not collected from the beginning of July through to the end of November.

FLOW AND TRANSPORT MODELLING

WATER FLOW

Analysis of tensiometer data showed that lateral flow can be neglected in comparison to vertical flow (Nützmann and Tischner, 2000). Therefore, a one-dimensional model was chosen to simulate field water transport. Water movement in unsaturated soil is described by Richards's equation

$$C(h) \frac{h}{t} - \frac{\partial}{\partial z} K(h) \frac{h}{z} = 1 - S \quad [1]$$

where: h is pressure head [L], C is differential water capacity [L^{-1}], K is hydraulic conductivity [L/T], S is volumetric root water uptake rate [T^{-1}], z is the space coordinate [L], increasing downwards, and t is time [T].

Vertical unsaturated/saturated water flow was calculated in the soil profile of 200 cm depth with the step $\Delta z = 2 \text{ cm}$, using the *HYDRUS 1D* software package (Simunek et al., 2005).

As initial conditions, we applied the measured pressure head at the beginning of the experiment. Boundary conditions include the measured pressure head at the bottom of the soil profile and the net water balance on the soil surface. The sink term S describes the rate of water uptake by roots. Potential evapotranspiration is calculated from hydro-climatic measurements using Penman's formula (DVWK, 1996). Actual evapotranspiration is dependent on the distribution of water pressure head in the soil and on root density. Water uptake by plants is described by the Feddes formula (Feddes et al., 1978, 2001):

$$S = b(h) \frac{ET^{pot}}{L_r} \quad [2]$$

where: $b(h)$ is the effectiveness of water uptake by roots [-], ET^{pot} is the potential transpiration [LT^{-1}], and L_r is the root length [L].

For the effectiveness function $b(h)$ the following distribution is assumed: plants start water uptake if the pressure head is smaller than a value of h_1 . Maximum water uptake equal to potential transpiration appears for pressure head between h_2 and h_3 . If the pressure head in the soil is smaller than h_3 , water uptake by roots decreases and is equal to zero at the point of permanent

wilting h_4 . From Dirksen et al. (1993) we adopted values for grass as $h_1 = -10 \text{ cm}$, $h_2 = -200 \text{ cm}$, $h_3 = -800 \text{ cm}$, $h_4 = -8000 \text{ cm}$.

Root density is changed with depth, following Dirksen et al. (1993). Between 10 and 40 cm depth we assumed a maximum root density, while from the soil surface to 10 cm depth and from 40 to 60 cm depth the density is 20% of the maximum.

The unsaturated soil profile consists of four layers. Hydraulic parameters of each layer, such as residual water content θ_r [$\text{L}^3 \text{L}^{-3}$], saturated water content θ_s [$\text{L}^3 \text{L}^{-3}$], saturated hydraulic conductivity K_s [LT^{-1}], and the parameters b [L^{-1}] and n [-] can be described by the Mualem and van Genuchten model (Kutilek and Nielsen, 1994). Hydraulic parameters of the soil were measured in the laboratory, and the results are shown in Table 1 (Berg et al., 2001). A comparison of *HYDRUS 1D* simulated values with measured values of pressure head during the experiment is shown in Figure 2. Without any parameter optimization we obtained a sufficient agreement between calculated and measured tensions in the soil, except at a depth of 30 cm. However, the time-dependence of pressure head variations at this depth is simulated moderately well. Simulation of water movement indicates that the distribution of pressure head, especially in the upper soil layer, is mainly affected by evapotranspiration. From the simulated spatial and temporal distribution of pressure head, water content throughout the soil profile can be calculated. Finally, water velocity is estimated using Darcy's law to provide a basis for solute transport modelling.

Table 1

Hydraulic parameters of the field soil column

Soil layer	Depth [cm]	θ_r [cm^3/cm^3]	θ_s [cm^3/cm^3]	b [mbar^{-1}]	n	K_s [cm/d]
1	0–30	0.06	0.31	0.024	2.11	9.6
2	30–60	0.06	0.33	0.017	3.37	14.4
3	60–90	0.04	0.32	0.018	4.54	12.0
4	90–200	0.03	0.35	0.024	4.58	72.0

θ_r – residual water content; θ_s – saturated water content; α , n – empirical parameters; K_s – saturated hydraulic conductivity

SOLUTE TRANSPORT

Tracer transport is described by the hydrodynamic advection-dispersion equation:

$$\frac{\partial C}{\partial t} - \frac{\partial}{\partial z} D \frac{\partial C}{\partial z} = v C \quad [3]$$

where: C is the tracer concentration [ML^{-3}], v represents the average velocity [LT^{-1}], and D is the dispersion coefficient in the liquid phase [$\text{L}^2 \text{T}^{-1}$], formulated by

$$D = \alpha_L v + D_d \quad [4]$$

where: α_L is the dispersivity [L] and D_d is the molecular diffusion coefficient in ground water [$\text{L}^2 \text{T}^{-1}$].

We solved Equation [3] numerically using *HYDRUS 1D*. As an initial condition, we assumed a constant concentration $C(z,0) = C_0$ (C_0 is the so-called background concentration, which is assumed to be 0 mg l^{-1} for bromide and 120 mg l^{-1} for deuterium). Boundary conditions were assumed as zero tracer

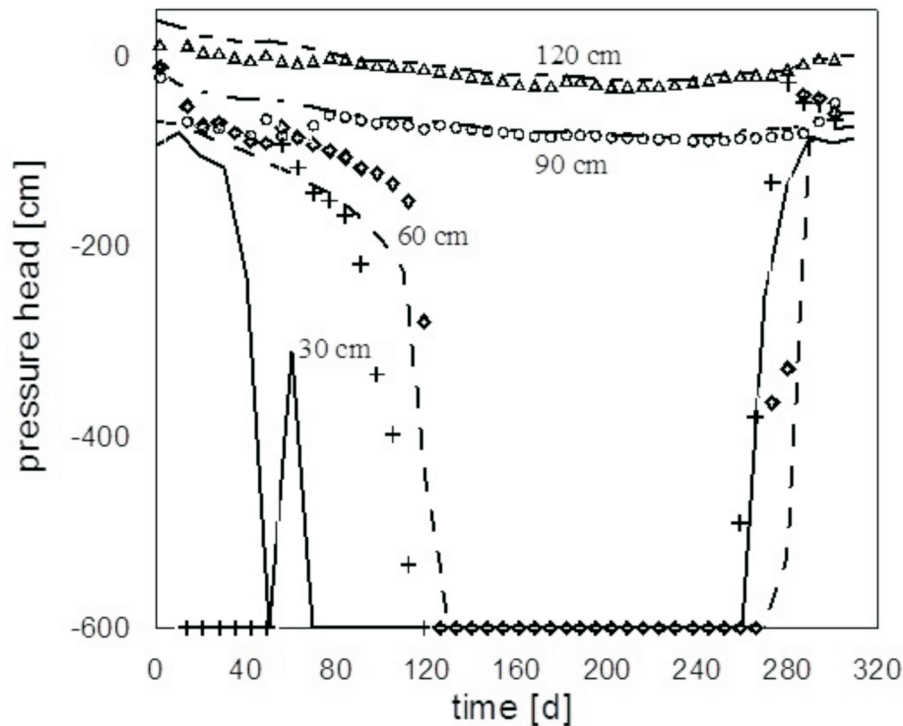


Fig. 2. Measured (points) and calculated (lines) pressure head distribution during tracer experiment for different depths

flux through the upper boundary and applying a zero concentration gradient at the bottom boundary.

In contrast to the unsaturated water flow model outputs discussed above, deterministic transport simulation results differ significantly from the measured bromide and deuterium concentrations. Furthermore, the measured BTC (breakthrough curve) at the same depths for location IIA and IIB, and IIIA and IIIB, are not really comparable, and, in some cases a higher maximum concentration at the depth of 60 cm than at the depth of 30 cm was observed. Concentration measurements have shown that the flow of groundwater takes place through many independent pathways.

This indicates that concentration measurements at one point in the field containing information about local water velocity or local volumetric moisture distribution cannot be adequately reproduced by deterministic modelled tracer transport with mean parameters.

A similar behaviour of a conservative solute transported in an unsaturated soil under steady-state flow conditions was observed for an experimental study of dependence of hydrodynamic dispersion on water content and water velocity fluctuation carried out in a large soil column (Nützmann et al., 2002). Using the hydrodynamic dispersion Equation [3] and a proposed relationship between dispersivity α_L and water flow velocity fluctuation, \tilde{v}_L (the authors obtained a close agreement of their numerical solutions to the experimental results).

Because, in the field experiment, a variation of the maximum concentration measured at the same depth but at different observation points for both tracers was observed, it could be hypothesized that this may occur mainly due to a high fluctuation of soil water velocity. Thus, the following questions must be answered: (1) how are dispersivity coefficients for the soil layers to be estimated, and, (2) how can field tracer transport be modelled based on these coefficients and point measurements?

RESULTS

ESTIMATION OF LOCAL TRANSPORT PARAMETERS FROM BTCS

Among the most important information obtained from tracer field measurements is fluctuation of water velocity (Jury and Fluehler, 1992; Nützmann et al., 2002; Nichol et al., 2005; Zhang and Xu, 2020; Jiménez-Martínez et al., 2020). This information is useful for both deterministic and stochastic descriptions of solute transport.

Measured concentration distributions at individual measuring points were used to estimate local groundwater flow rates and local hydrodynamic dispersion parameters. In a first step we estimate the mean daily water velocity \bar{v} and dispersivity α_L separately for each observation point. Then, calculated breakthrough curves are obtained as solutions of the advection-dispersion Equation [3] assuming that the dispersion coefficient is described by Equation 4, which is solved using the Monte Carlo method (random walk model) and the following initial and boundary conditions:

- initial condition $C(z,0) = C_0$ (C_0 is the background concentration),
- boundary conditions:
 - $t = 0$ and $z = 0$ (soil surface): injected mass of tracer equals M , a Dirac impulse.
 - $t > 0$ and $z = 0$: impermeable screen.
 - $t > 0$ and $z = L$ (L is the depth of soil profile): permeable screen.

The random walk model (Bechtold et al., 2011) is based on modelling of the motion of artificial particles of a solute. The tracer mass M is divided into N artificial particles. The change in the position of particle number i in time Δt was calculated using the equation:

$$c_i(t) = c_i(t) + \sqrt{2D} \frac{v(t)}{t} N(0,1) \quad [5]$$

where: $v(t)$ is the water velocity in time t , D is the coefficient of hydrodynamic-dispersion, $N(0,1)$ is the random variable having a standard normal distribution (expected value = 0 and standard deviation = 1).

Considering a Representative Elementary Volume in the unsaturated zone, the tracer concentration $C = m/V$ is proportional to the particle concentration $C^p = n/V$, where n is the number of particles corresponding to the tracer mass m dissolved in a volume V of soil water. The ratio of the tracer concentration to particle concentration is constant and equals $C/C^p = m/n = M/N$. Using the last formula we evaluated the real mass of the tracer taking part in motion as $M = NC_{max}^p/C_{max}$, where: C_{max} is the maximum measured concentration and C_{max}^p is the maximum concentration of particles.

As an upper boundary condition, a tracer surface concentration at time $t = 0$ was assumed. This concentration is $C_{surf} = M/S$, where S is the area of injection. This boundary condition was separately estimated for each breakthrough curve. Consistency of calculated maximum tracer concentration to measured maximum concentration was used as a criterion of correctness of boundary condition setting. The parameters were changed until theoretical breakthrough curves were compatible with the measurement data. The local groundwater flow velocity was correlated with measured precipitation rates.

The injected tracer concentrations were for bromide $46.6 \text{ g}/10 \text{ m}^2 = 0.466 \text{ mg cm}^{-2}$ and for deuterium 5.55 mg cm^{-2} . For these values, the best compatibility of measurement and calculation results was obtained.

Figures 3 and 4 show that measured and calculated BTCs for both tracers compared well. These results show that for each observation point we can estimate the flow velocity as a

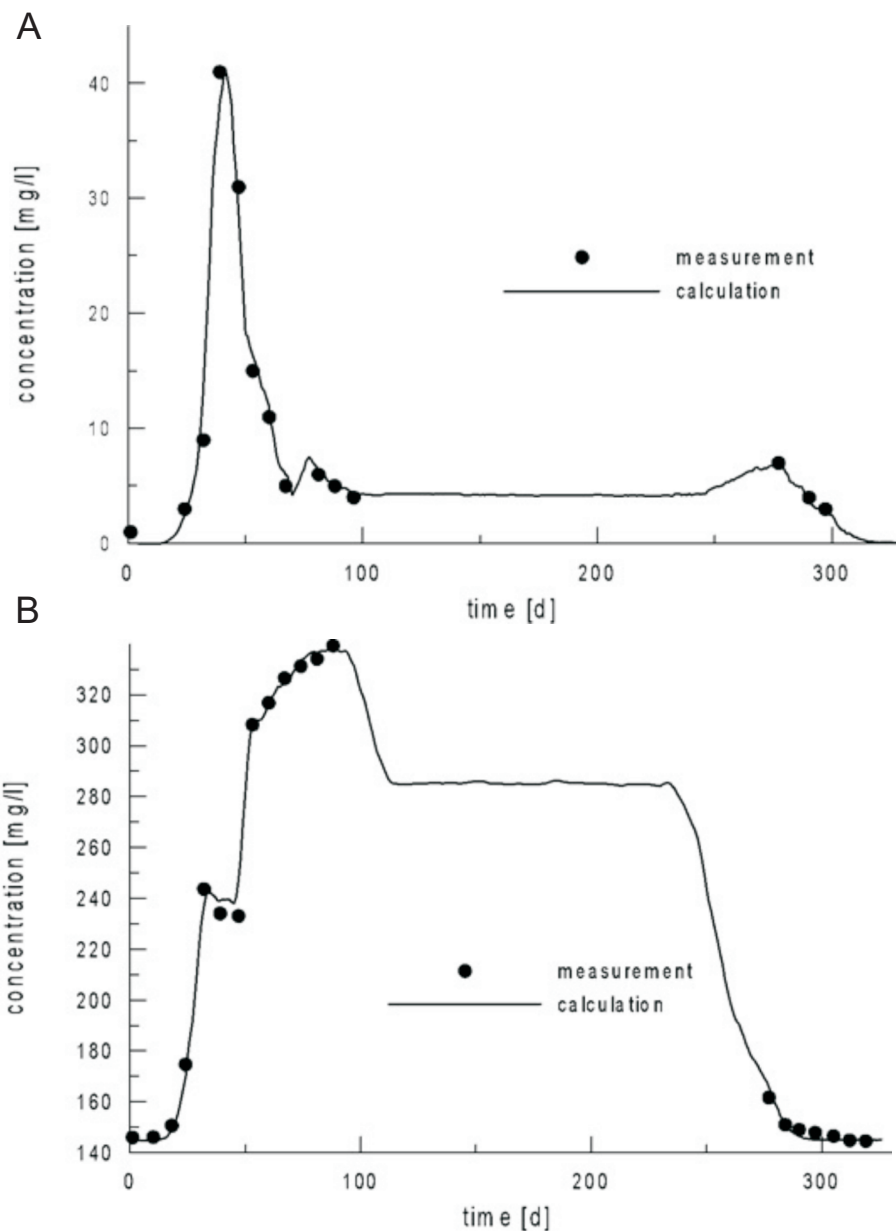


Fig. 3A – comparison of measured and simulated bromide breakthrough at 30 cm depth (location II A); B – comparison of measured and simulated deuterium breakthrough at 30 cm depth (location II B)

function of time and dispersivity describing tracer movement only in this location very well. The fitted dispersivity values for all measurement points and for both tracers are given in Tables 2 and 3. They vary from 0.09 to 0.6 cm for bromide and from 0.32 to 2.1 cm for deuterium. In the calculations, it was assumed that the infiltrating water flows in single paths without exchange with the environment.

The difference between the initial actual concentration and the concentration assumed in the calculation shows how much of the tracer leaves a single flow path. During the natural flow, mixing is carried out not only in the direction of the flowing stream, but transverse mixing also occurs.

Groundwater is taken up by the roots of plants. Along with groundwater, one of the tracers, i.e. deuterium, is taken up. Therefore, it is difficult to compare the concentrations of both markers even at the same sampling point.

This is the cause for these estimated surface tracer concentrations – shown in Tables 2 and 3 – being ~20% of the real injected tracer concentrations for both solutes, bromide and deuterium.

Estimated water velocities in the soil for all measurement points are shown in Figure 5A. Thin lines show water velocity as a function of time, calculated from twelve measured breakthrough curves; the thick line shows the resulting mean water

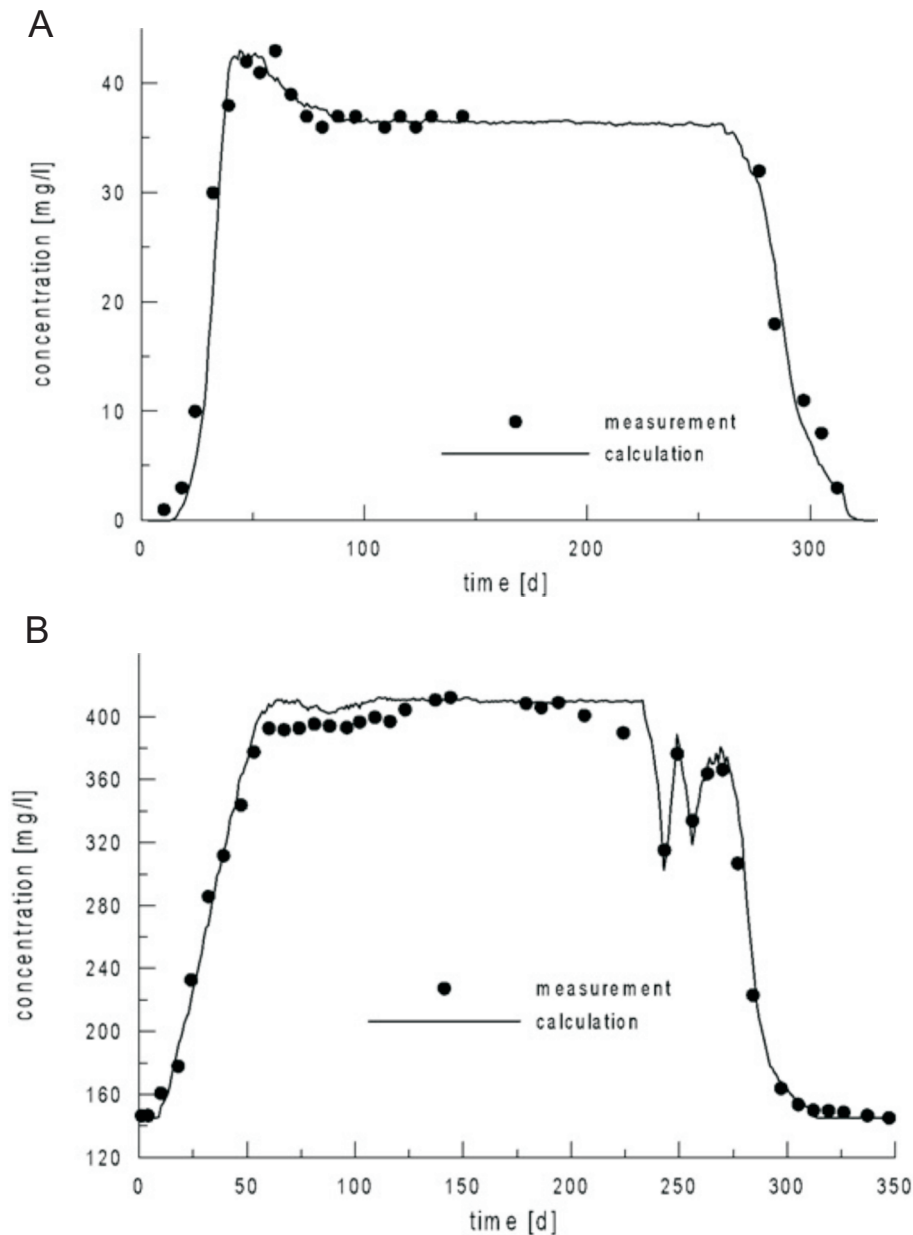


Fig. 4A – comparison of measured and simulated bromide breakthrough at 60 cm depth (location II A); B – comparison of measured and simulated deuterium breakthrough at 60 cm depth (location II B)

Table 2

Dispersivities and initial surface tracer concentrations identified from bromide BTCs

Measurement point	Depth [cm]	Dispersivity [cm]	Estimated initial surface concentration [mg/cm ²]
30	30	0.6	0.1232
30A	30	0.55	0.1352
60	60	0.2	0.1308
60A	60	0.282	0.1236
60B	60	0.09	0.1248
90	90	0.024	0.123

Table 3

Dispersivities and initial surface tracer concentrations identified from deuterium BTCs

Measurement point	Depth [cm]	Dispersivity [cm]	Estimated initial surface concentration [mg/cm ²]
30	30	2.1	1.0788
30A	30	0.55	1.0416
60	60	0.38	1.0064
60A	60	0.512	1.0432
60B	60	0.32	1.0328
90	90	0.35	1.0308

velocity and velocity standard deviation in Figure 5B. It is obvious that a high fluctuation of water velocity in the soil profile occurs, which could explain the observed earlier breakthroughs in deeper sampling points than in shallow ones.

STOCHASTIC MODEL OF SOLUTE TRANSPORT IN THE SOIL PROFILE

Assuming that soil water is flowing by a number of independent pathways, we can define a simple stochastic model for the transport of tracer particles as shown schematically in Figure 6. The tracer particle velocity for a single pathway with the number i can be described by the following stochastic equation:

$$v_i(t) = \bar{v} + \Delta v N(0,1) \quad (6)$$

where: \bar{v} is the mean water velocity, Δv is the standard deviation of water velocity, t is time, and $N(0,1)$ is a normally distributed random variable with a mean value 0 and a standard deviation of 1.

Now, tracer transport along a pathway j can be described by dividing the mass of the applied tracer into a number of virtual particles i and using a random walk model to describe the change of the position of each particle during a time step Δt .

$$z_{ij}(t + \Delta t) = z_{ij}(t) + v_i(t) \Delta t \quad (7)$$

where: $z_{ij}(t)$ is the position of the particle at time t , $z_{ij}(t + \Delta t)$ the position of the particle at time $t + \Delta t$, j is the particle number which is transported by flow path number i .

A particle's displacement from time t to $t + \Delta t$ is caused by advection and dispersion following Equation [8]

$$z_{ij}(t + \Delta t) = z_{ij}(t) + v_i(t) \Delta t + \sqrt{2D} N(0,1) \Delta t \quad (8)$$

where: $v_i(t)$ is described by Equation [6].

Thus, breakthrough curves measured at different observation points are considered as a single realization of a defined stochastic process for one pathway. The mean concentration C

of tracer at depth z in the soil profile for a single realization of the stochastic model is:

$$C(z,t) = \frac{1}{N_p} \sum_{i=1}^{N_p} C_i(z,t) \quad [9]$$

where: N_p is the number of different pathways and C_i is the concentration of tracer for the i -th pathway.

To illustrate the differences between the deterministic model described by the hydrodynamic dispersion Equation [3], and the proposed stochastic model, some simulations are presented. The simulations with this stochastic model were carried out including more than 1000 flow pathways. For comparison, the deterministic model (3) was applied with the above-calculated mean daily velocities and α value of dispersivity, which can best describe dispersion and mixing effects caused by fluctuations of water velocity during flow through a set of pathways. In the test case described, the relative fluctuations of water velocity are fixed to 0.1, 0.25 and 0.4, the mean water velocity is $v = 1 \text{ cm d}^{-1}$. For the stochastic model we assumed that dispersivity for a single pathway is to 0.3 cm (it was the most frequent value for all measured points, see Tables 2 and 3).

For each case we found, by systematic variation of the dispersivity, a value giving the best agreement between the simulated BTCs of both models. Calculated results are depicted in Figure 7. They show that for a relative water velocity fluctuation of 0.1 the mean BTCs described by stochastic and deterministic models are similar. In such a case we can use the deterministic model with a higher dispersivity than for a single pathway for simulating the mean tracer breakthrough; for the case described here it was $\alpha_L = 0.775 \text{ cm}$. If the relative fluctuation of water flow velocity increases, the differences between both models also increase. This means that for higher heterogeneity of water flow velocity, the deterministic dispersion model does not properly describe tracer transport. Such a situation is recognized in the field experiment if the relative fluctuation of water flow velocity is higher than 1 (see Fig. 5A).

Using the stochastic model described by equations 5–8, theoretical mean breakthrough curves for bromide are simulated for depths of 30, 60 and 90 cm (Fig. 8). Here we used values of mean daily water velocity $\bar{v}(t)$ and standard deviation from $\Delta v(t)$ experimental data which are shown in Figures 5A,

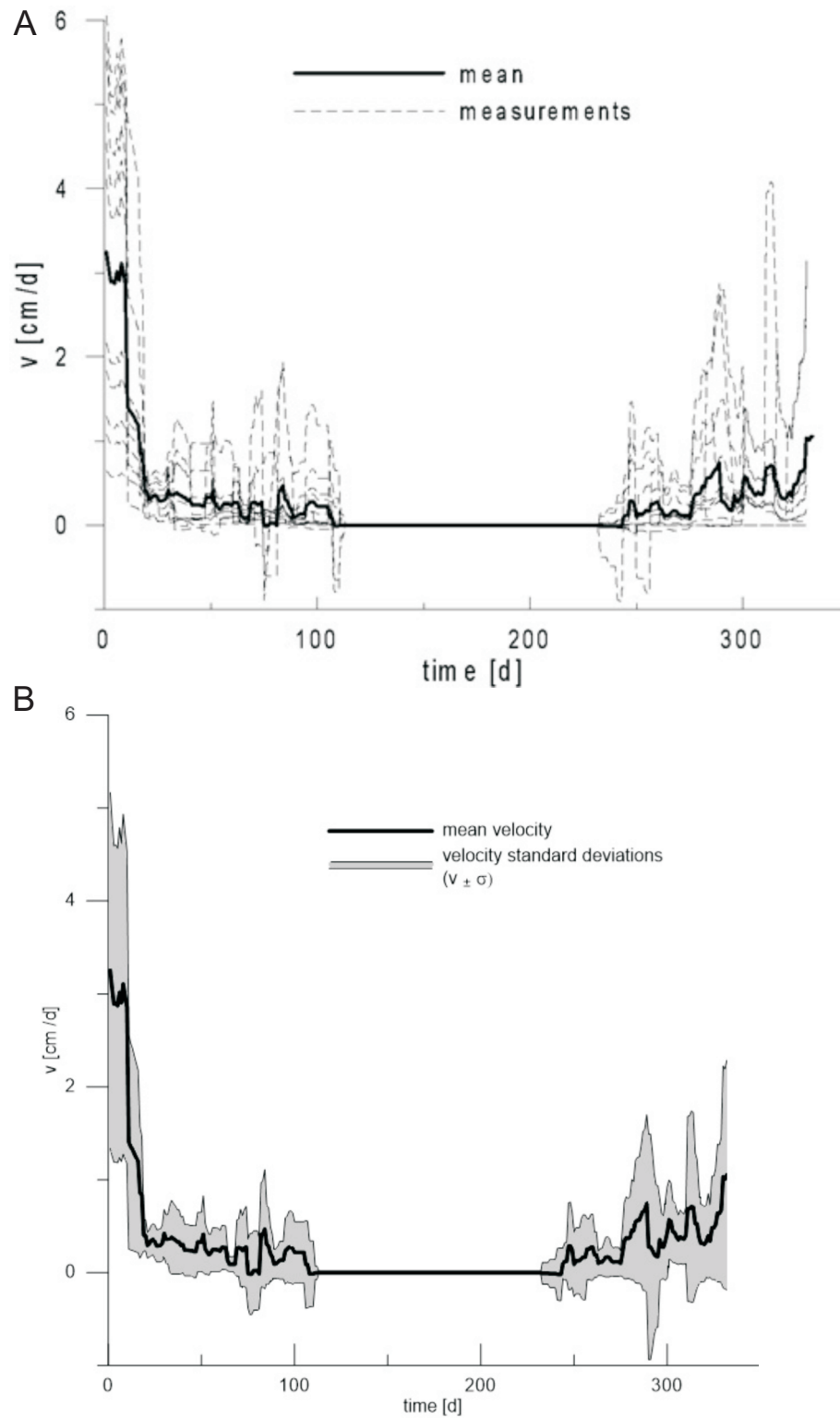


Fig. 5A – Estimated water velocity in field soil profile; B – estimation of velocity standard deviation

B. These results describe an average tracer transport through the experimental soil profile. Additionally, we compared these BTCs to deterministic simulation results with mean daily water velocity. Results shown in Figure 9 illustrate tracer transport through a single pathway with mean water velocity and, in contrast to the stochastic simulation, they do not accurately describe mixing caused by water velocity fluctuations in the soil

profile. Based on the calculations presented, we can estimate the local flow rates of groundwater in the unsaturated zone and the longitudinal dispersion coefficient in a given flow path.

The simulation results shown in Figures 8 and 9 show the mean behaviour of the tracer cannot be compared with any experimental BTC. Such comparisons for local example transition curves are presented when discussing the results of measure-

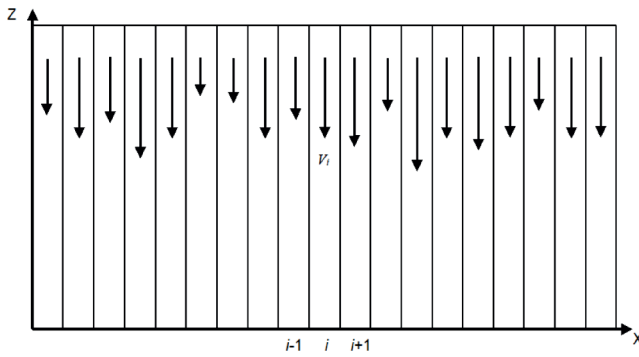


Fig. 6. Scheme of the stochastic model concept with independent flow pathways

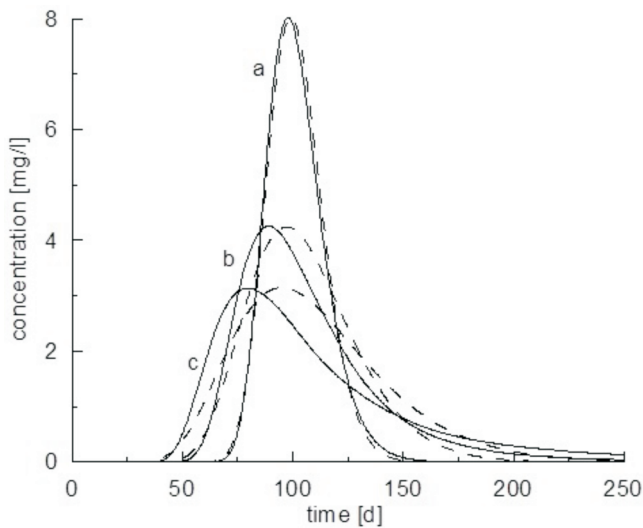


Fig. 7. Comparison of stochastic model and dispersion model

Solid line: for $v/v = 0.1$ (a), 0.25 (b), 0.4 (c); dashed line for different dispersivities $\alpha = 0,775$ (a), 2.8 (b), 5.15 (c) cm

ments. Substances that enter groundwater from the surface flow through the unsaturated zone. Estimating the inflow of substances to groundwater in a saturated zone requires a reliable transport model through the unsaturated zone.

The results of the experiments described show that transport in the unsaturated zone takes place along many independent flow paths with a large variation in flow rate.

The stochastic model presented, taking into account the actual fluctuations of groundwater velocity, better describes on a field scale the average transport of substances entering from the ground surface through the unsaturated zone to the saturated zone.

CONCLUSIONS

Based on spatially and temporally distributed field measurements of pressure head in the unsaturated zone and break-

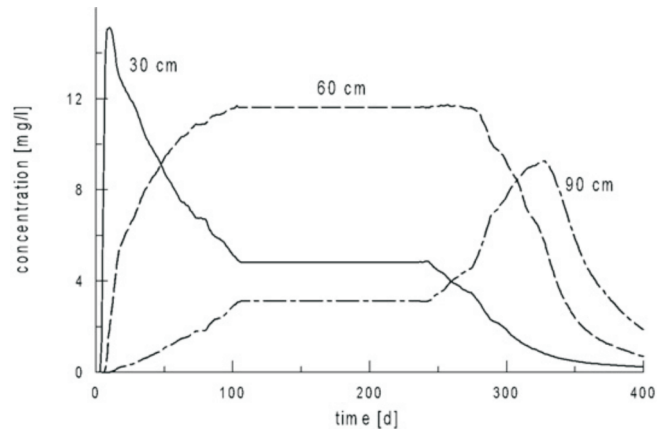


Fig. 8. Theoretical expected breakthrough curves for bromide (stochastic model)

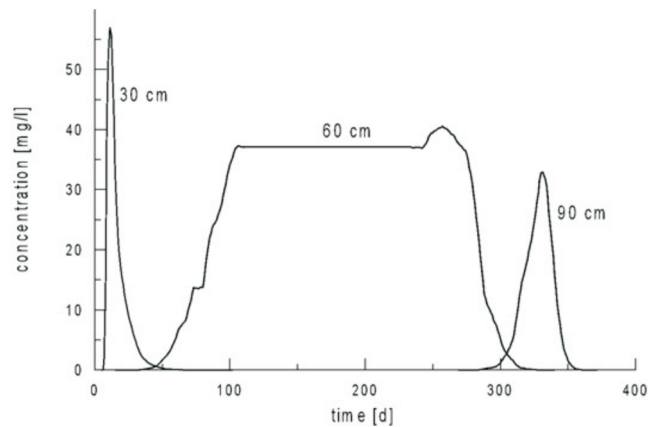


Fig. 9. Theoretical expected breakthrough curves for bromide (deterministic model with a mean water velocity)

through data from a dual tracer experiment, we have tried to answer the question of how best to model tracer transport in this case. Because lateral flow could be neglected, one-dimensional vertical tracer transport was simulated using the classical advection-dispersion equation and a stochastic approach. Connected with this was the problem of estimating the dispersivity as a mean value for the advection-dispersion equation or as a water velocity-dependent parameter varying with the fluctuation of flow velocity during the experiment.

Similarly to a soil column study (Nützmann et al., 2002) we found that the concept of solute transport in an unsaturated soil which takes place by numerous independent flow pathways, each of which is represented by a single flow velocity, is generally applicable. Because of the assumed stochastic nature of water flow in the vadose zone, it is impossible to determine mean dispersivity from in situ measurements at single observation points. Tracer breakthrough curves measured at one point do not give representative information concerning hydrodynamic dispersion. These breakthrough curves show water velocity at a measurement point. Using this information and a large number of realisations (which means independent flow paths) stochastic modelling also seems to be an adequate method for simulating tracer transport at the field scale. If the

fluctuation in the unsaturated water flow velocity is small, stochastic and deterministic modelling results become similar, but with increased velocity fluctuation the differences between both models also increase. The measurements presented showed large fluctuations of groundwater velocity. In this case, only the stochastic model correctly describes the mean movement of the tracer.

The advantage of the stochastic modelling method proposed here for field-scale tracer application is to produce reliable information about expected total solute fluxes from the unsaturated zone to groundwater, or mean transit times. Moreover, this allows one to evaluate the mass of solute in the soil profile and to determine the range of water velocity fluctua-

tions. Field experiments should be concentrated on estimation of fluctuations of water flow velocity to make stochastic models more accurate.

Acknowledgements. The authors are grateful to the DAAD bilateral programme between Poland and Germany for supporting this research financially. They also wish to thank Dr W. Stichler from the Institute of Groundwater Ecology, Helmholtz-Centre Munich, for his assistance with field measurements. The authors would like to thank the reviewers for their thoughtful comments and efforts towards improving this manuscript.

REFERENCES

- Amoozegard-Fard, A., Nielsen, D.R., Warrick, A.W., 1982.** Soil solute concentration distributions for spatial varying pore-water velocities and apparent diffusion coefficients. *Soil Science Society of America Proceedings*, **46**: 3–8.
- Bechtold, M., Vanderborght, J., Ippisch, O., Vereecken, H., 2011.** Efficient random walk particle tracking algorithm for advective-dispersive transport in media with discontinuous dispersion Coients and water content. *Water Resources Research*, **47**: W10526.
- Berg, W., Cencur, B., Fank, J., Feichtinger, F., Nützmann, G., Papesch, W., Rajner, V., Rank, D., Schneider, S., Seiler, K.-P., Steiner, K.-H., Stenitzer, E., Stichler, W., Trcek, B., Vargay, Z., Veselic, M., Zojer, H., 2001.** Tracers in the unsaturated zone. *Beiträge zur Hydrogeologie*, **52**: 7–102.
- Berkowitz, B., Scher, H., 1995.** On characterization of anomalous dispersion in porous and fractured media. *Water Resources Research*, **31**: 1461–1466.
- Biggar, J.W., Nielsen, D.R., 1976.** Spatial variability of the leaching characteristics of a field soil. *Water Resources Research*, **12**: 78–84.
- Bromly, M., Hinz, C., 2004.** Non-Darcian transport in homogeneous unsaturated repacked sand. *Water Resources Research*, **40**: W07402.
- Butters, G.L., Jury, W.A., Ernst, F.F., 1989.** Field scale transport of bromide in an unsaturated soil 1. Experimental methodology and results. *Water Resources Research*, **25**: 1575–1581.
- Chan, T.P., Govindaraju, R.S., 2006.** A stochastic-advective transport model for NAPL dissolution and degradation in non-uniform flows in porous media. *Journal of Contaminant Hydrology*, **87**: 253–276.
- Claes, N., Ginger Paige, G., Parsekian, A.D., 2019.** Uniform and lateral preferential flow under flood irrigation at field scale. *Hydrological Processes*, **33**.
- Cortis, A., Berkowitz, B., 2004.** Anomalous transport in "classical" soil and sand columns. *Soil Science Society of America Journal*, **68**: 1539–1548.
- Dagan, G., Bresler, E., 1979.** Solute dispersion in unsaturated heterogeneous soil at field scale, I. Theory. *Soil Science Society of America Journal*, **43**: 461–467.
- Dirksen, C., Kool, J.B., Koorevaar, P., van Genuchten, M.Th., 1993.** HYWASOR – Simulation model of hysteretic water and solute transport in the root zone. In: *Water Flow and Solute Transport in Soils* (eds. D. Russo and G. Dagan): 99–122. Springer, Berlin.
- DVWK, 1996.** Ermittlung der Verdunstung von Land- und Wasserflächen. *Merkblätter zur Wasserwirtschaft*, **238**.
- Feddes, R.A., Kowalik, P., Zaradny, H., 1978.** *Simulation of Field Water Use and the Crop Yield*. John Wiley and Sons, New York-Toronto.
- Feddes, R.A., Hoff, H., Bruen, M., Dawson, T., de Rosnay, P., Dirmeyer, P., Jackson, R.B., Kabat, P., Kleidon, A., Lilly, A., Pitman, A.J., 2001.** Modelling root water uptake in hydrological and climate models. *Bulletin of the American Meteorological Society*, **82**: 2797–2809.
- Fried, J.J., 1975.** *Groundwater Pollution*. Elsevier Science, New York.
- Hammel, K., Gross, J.M., Wessolek, G., Roth, K., 1999.** Two-dimensional simulation of bromide transport in a heterogeneous field soil with transient unsaturated flow. *European Journal of Soil Science*, **50**: 6333–647.
- Huang, K., Toride, N., van Genuchten, M.Th., 1995.** Experimental investigation of solute transport in large, homogeneous and heterogeneous, saturated soil columns. *Transport in Porous Media*, **18**: 283–302.
- Jaynes, D.B., Bowman, R.C., 1988.** Transport of conservative tracer in the field under continuous flood irrigation. *Soil Science Society of America Journal*, **52**: 618–624.
- Jiménez-Martínez, J., Alcolea, A., Straubhaar, J.A., Renard, P., 2020.** Impact of phases distribution on mixing and reactions in unsaturated porous media. *Advances in Water Resources*, **144**: 103697.
- Jury, W.A., Fluehler, H., 1992.** Transport of chemicals through soils: Mechanisms, models and field applications. *Advances in Agronomy*, **47**: 141–201.
- Kutilek, M., Nielsen, D.R., 1994.** *Soil Hydrology*. Cremlingen – Destect, Catena-Verlag.
- Li, X., Wen, Z., Zhan, H., Wu, F., Qi Zhu, Q., 2021.** Laboratory observations for two-dimensional solute transport in an aquifer-aquitard system. *Environmental Science and Pollution Research*, **28**: 38664–38678.
- Moroni, M., Kleinfelder, N., Cushman, H., 2007.** Analysis of dispersion in porous media via matched-index particle tracking velocimetry experiments. *Advances in Water Resources*, **30**: 1–15.
- Nichol, C., Smith, L., Beckie, R., 2005.** Field-scale experiments of unsaturated flow and solute transport in a heterogeneous porous medium. *Water Resources Research*, **41**: W05018.
- Nützmann, G., Maciejewski, S., 2002.** Modelling studies for determining unsaturated flow components in a sandy soil during dual tracer test. *Developments in Water Science*, **47**: 33–40.
- Nützmann, G., Tischner, T., 2000.** Phosphorverlagerung im Boden: physikochemische und hydrologische Einflüsse. *Mitteilungen Deutsche Bodenkundliche Gesellschaft*, **92**: 182–185.

- Nützmann, G., Maciejewski, S., Joswig, K., 2002.** Estimation of water saturation dependence of dispersion in unsaturated porous media: experiments and modeling analysis. *Advances in Water Resources*, **25**: 565–576.
- Pachepsky, Y., Benson, D., Rawls, R., 2000.** Simulating scale-dependent contaminant transport in soils with the fractional advective-dispersive equation. *Soil Science Society of America Journal*, **64**: 1234–1243.
- Raimbault, J., Peyneau, P.-E., Courtier-Murias, D., Bigot, T., Roca, J.G., Bechet, B., Lassabatere, L., 2021.** Investigating the impact of exit effects on solute transport in macroporous media. *Hydrology and Earth System Sciences, European Geosciences Union*, **25**: 671–683.
- Siliman, S.E., Simpson, E.S., 1987.** Laboratory evidence of the scale effect in dispersion of solutes in porous media. *Water Resources Research*, **23**: 1667–1673.
- Simunek, J., Sejna, M., van Genuchten, M.T., 2005.** The HYDRUS-1D software package for simulating the one-dimensional movement of water, heat and multiple solutes in variably-saturated media, Riverside, California.
- Tilahun, K., Botha, J.F., Bennie, A.T.P., 2005.** Transport of bromide in the Bainsvlei soil: field experiment and deterministic/stochastic model simulation. I. Continuous water application. *Australian Journal of Soil Research*, **43**: 73–80.
- Tischner, T., 2000.** Untersuchungen zur Phosphatverlagerung und Phosphatbindung im Boden und Grundwasser einer landwirtschaftlich genutzten Fläche. *Bodenökologie und Bodengeneese*, (33): 187.
- Toride, N., Leij, F.J., 1996a.** Convective-dispersive stream tube model for field scale solute transport: I. Moment analysis. *Soil Science Society of America Journal*, **60**: 342–352.
- Toride, N., Leij, F.J., 1996b.** Convective-dispersive stream tube model for field scale solute transport: I. Moment analysis. *Soil Science Society of America Journal*, **60**: 352–361.
- Wessolek, G., Gross, J.M., Hammel, K., 2000.** Water and bromide transport in heterogeneous glacial sand. *Journal of Plant Nutrition and Soil Science*, **163**: 13–20.
- Xiong, Y., Huang, G., Huang, Q., 2006.** Modeling solute transport in one-dimensional homogeneous and heterogeneous soil columns with continuous time random walk. *Journal of Contaminant Hydrology*, **86**: 163–175.
- Yeh, T.C.J., 1987.** Comment on “Modeling of-scale dependent dispersion in hydrogeologic systems.” By J. F. Pickens and G. E. Grisak. *Water Resources Research*, **23**: 522.
- Zhang, W.J., Xu, X.-B., 2020.** Experimental study on migration of chloride ion and cadmium ion in unsaturated soil. *Journal of Environmental Geotechnics*. Published online: <https://doi.org/10.1680/jenge.20.00014>.